The initiation and evolution of the River Nile

Laura Fielding [a], Yani Najman [a,*], Ian Millar [b], Peter Butterworth [c], Eduardo Garzanti [d], Giovanni Vezzoli [d], Dan Barfod [e], Ben Kneller [f]

[a] *Lancaster Environment Centre, Lancaster University, Lancaster, UK*
[b] *British Geological Survey, Keyworth, UK*
[c] *BP Egypt, Cairo, Egypt*
[d] *University Milano-Biccoca, Milan, Italy*
[e] *SUERC, East Kilbride, UK*
[f] *University of Aberdeen, Aberdeen, UK*

ARTICLE INFO

ABSTRACT

The Nile is generally regarded as the longest river in the world. Knowledge of the timing of the Nile's initiation as a major river is important to a number of research questions. For example, the timing of the river's establishment as a catchment of continental proportions can be used to document surface uplift of its Ethiopian upland drainage, with implications for constraining rift tectonics. Furthermore, the time of major freshwater input to the Mediterranean is considered to be an important factor in the development of sapropels. Yet the river's initiation as a major drainage is currently constrained no more precisely than Eocene to Pleistocene.

Within the modern Nile catchment, voluminous Cenozoic Continental Flood Basalts (CFBs) are unique to the Ethiopian Highlands; thus first detection of their presence in the Nile delta record indicates establishment of the river's drainage at continental proportions at that time. We present the first detailed multiproxy provenance study of Oligocene–Recent Nile delta cone sediments. We demonstrate the presence of Ethiopian CFB detritus in the Nile delta from the start of our studied record (c. 31 Ma) by (1) documenting the presence of zircons with U–Pb ages unique, within the Nile catchment, to the Ethiopian CFBs and (2) using Sr–Nd data to construct a mixing model which indicates a contribution from the CFBs. We thereby show that the Nile river was established as a river of continental proportions by Oligocene times. We use petrography and heavy mineral data to show that previous petrographic provenance studies which proposed a Pleistocene age for first arrival of Ethiopian CFBs in the Nile delta did not take into account the strong diagenetic influence on the samples.

We use a range of techniques to show that sediments were derived from Phanerozoic sedimentary rocks that blanket North Africa, Arabian–Nubian Shield basement terranes, and Ethiopian CFB's. We see no significant input from Archaean cratons supplied directly via the White Nile in any of our samples. Whilst there are subtle differences between our Nile delta samples from the Oligocene and Pliocene compared to those from the Miocene and Pleistocene, the overall stability of our signal throughout the delta record, and its similarity to the modern Nile signature, indicates no major change in the Nile's drainage from Oligocene to present day.

1. Introduction

The Nile is generally regarded as the longest river in the world, stretching >6800 km across the length of north-eastern Africa. Its evolution has been used to date the timing of the region's surface uplift and hence constrain continental break-up tectonics (e.g. Paul et al., 2014). In addition, its runoff is proposed to have had a major influence on sapropel development in the Mediterranean (e.g. Krom et al., 2002; Meijer and Tuenter, 2007) and its delta plays host to a major hydrocarbon producing region. However, despite its clear importance, little is known of the river's evolution through time.

The present-day Nile has three main tributaries: the White Nile, the Blue Nile and the Atbara (Fig. 1). Sediment supplied to the Nile trunk in Egypt is dominated by contributions from the Blue Nile (50–61%) and Atbara (30–42%) (Padoan et al., 2011). The vast majority of White Nile sediment load is trapped in

* Corresponding author.
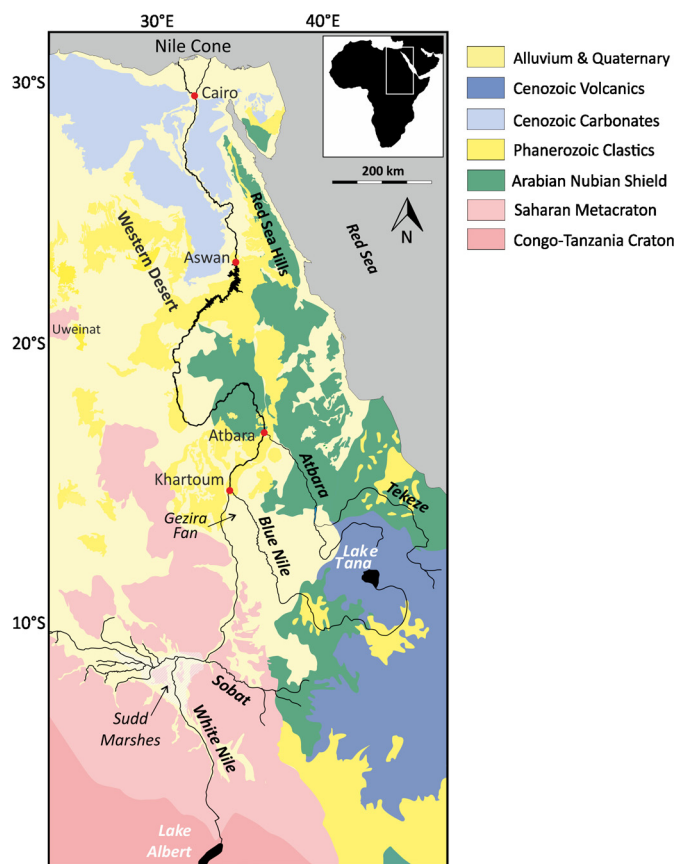 *E-mail address:* y.najman@lancs.ac.uk (Y. Najman).

Fig. 1. Geological map of the Nile drainage (modified from Fielding et al., 2017). (For interpretation of the colours in the figure(s), the reader is referred to the web version of this article.)

extensive swamps in South Sudan (the Sudd marshes, Fig. 1), and does not reach the main Nile trunk, thus accounting for <3% of the total sediment reaching the modern delta. Today, detritus supplied to the Nile trunk is derived from the volcanic Ethiopian Highlands, Precambrian basement rocks of the Arabian–Nubian Shield and Saharan Metacraton, and Phanerozoic sedimentary cover that blankets much of the region (Fig. 1), together with a contribution from aeolian sources (e.g. Fielding et al., 2017; Padoan et al., 2011). However, little is known about the past evolution of the Nile River, and the changing influences of tectonics and climate through time (Hamann et al., 2008; Paul et al., 2014; Pik et al., 2003; Woodward et al., 2015). There is no consensus as to when the river first initiated; ages of Oligocene (Gani et al., 2007; Pik et al., 2003) to Pleistocene (Macgregor, 2012; Shukri, 1949/1950) have been proposed for the time the Nile trunk river first drained as far south as the Ethiopian Highlands.

In this paper, we provide a range of analyses from a unique archive of offshore Nile delta sediments aged from 31–0 Ma. We use the data to: i) determine when the Nile river evolved from one of local catchment to a major river of continental proportions; ii) document the evolution of the river through time; iii) discuss the influence of the river runoff on sapropel development; and, iv) provide new evidence constraining the timing of Ethiopian plateau uplift, thus contributing to our understanding of Cenozoic African tectonics.

2. Approach and geological background

In this study, we use sediments from the Nile delta cone as a record of Nile evolution through time. Biostratigraphically dated samples were provided by BP Egypt. We studied samples from the

Oligocene between 31 and 27.5 Ma; from the Miocene between 17–15.2 Ma; from the Pliocene between 3.25 to 2.65 Ma; and from the Pleistocene at 1.3 Ma. We carried out isotopic, geochemical, petrographic and heavy-mineral analyses on the Nile delta cone samples in order to identify provenance changes through time. Comparisons are made with published data from potential Nile catchment source regions in the past, and with data from the modern Nile River.

2.1. The Nile delta cone

The earliest records of the delta are preserved onshore in Egypt near Fayoum, and have been dated as Eocene (38–35 Ma) (Salem, 1976; Underwood et al., 2013). The delta began to prograde north as the Tethys Ocean receded, depositing in its current offshore location from the Oligocene. Changes in sediment accumulation, composition, facies and architecture (Craig et al., 2011; Gardosh et al., 2009) are interpreted as initiation of major Nile drainage at 30 Ma, but this was not thought to extend as far south as the Ethiopian Highlands (Macgregor, 2012). Sediment accumulation continued in the Mediterranean until the end-Miocene Messinian Salinity Crisis (Dolson et al., 2001), after which the Zanclean flood rapidly filled the Mediterranean basin. An increase in sedimentation rate in the Nile delta cone during the Late Pliocene–Early Pleistocene is proposed by Macgregor (2012) to result from uplift of the Ethiopian Rift shoulders, with associated increased rainfall and erosion.

This study represents the first access to the deep sedimentary archive of the Nile delta for multi-proxy provenance analysis. Previous provenance studies have largely concentrated on the younger Plio-Pleistocene record. Previous mineralogical work (summarised in Macgregor (2012)) recorded a down-core decrease in detritus derived from the Ethiopian Continental Flood Basalts (CFBs), and interpreted this as a provenance signal indicating only a recent connection between the Blue Nile and the main trunk Nile. However, the influence of diagenesis on this record was not considered. Sr–Nd bulk-sample data, complemented by geochemical and/or clay mineralogy analyses, have also been used to assess Nile provenance over the recent geological past (e.g. Freydier et al., 2001; Krom et al., 2002; Revel et al., 2014). These studies inferred mixing between Blue Nile Ethiopian input and White Nile cratonic/Saharan aerosols. Such variations have been ascribed to alternating wetter and drier periods, potentially relating to shifting of the Inter Tropical Convergence Zone, and to climatic episodes such as the Last Glacial Maximum and African Humid Period.

In this study, we present the first detrital zircon U–Pb and Hf-isotope data for samples from the Nile delta cone. We also extend petrographic, heavy-mineral and Sr–Nd data as far back as the Oligocene, thus providing the first long-range provenance study of the delta. In addition to data from the Nile delta cone, we present the first detrital zircon U–Pb and hafnium isotope data for Saharan dune sands, in order to constrain the composition of aeolian input into Nile delta sediments.

2.2. Geology of the Nile River catchment and hinterland

The geology of the modern Nile catchment has largely been shaped by the events of the Pan-African Orogeny (Kröner and Stern, 2004), when east and west Gondwana collided to form 'Greater Gondwana' at the end of the Neoproterozoic. In North Africa, this orogeny involved the collision of ancient cratons such as the Congo–Tanzania craton and the Saharan Metacraton with juvenile oceanic island arcs of the Arabian Nubian Shield. Subsequent to that orogeny, erosion of the Trans-Gondwanan mountain belt and recycling of the eroded detritus during later inversion tectonics resulted in the deposition of a thick cover of flu-

vial and marine sediments overlying the amalgamated terrains, from the Cambrian onwards (e.g. Klitzsch and Squyres, 1990). Sedimentation continued, episodically, until Cenozoic times, influenced by various periods of tectonism. The most important of these tectonic events is the opening of Neotethys and later of the South Atlantic, which resulted in the development of rift basins in the region, with Late Cretaceous–early Eocene inversion of such basins due to the convergence of the Mediterranean with the African margin (Bosworth et al., 2008; Guiraud et al., 2005; Klitzsch and Squyres, 1990).

The evolution of the Nile has also been strongly controlled by the Cenozoic tectonic history of northeast Africa. Development of the East African rift (Ebinger, 2005), and uplift of the Nile source regions in the Ethiopian Highlands, has resulted in magmatism since Oligocene times (Pik et al., 2003), including eruption of voluminous continental flood basalts. Opening of the Red Sea rift led to uplift on the rift flanks facing the Nile basin in the Oligocene (Bosworth et al., 2005; Omar and Steckler, 1995).

Today, the White Nile is sourced from Lake Victoria in Uganda, and drains Archaean–Paleoproterozoic rocks of the Congo–Tanzania Craton. Further north it flows over the Saharan Metacraton (SMC), comprising Archaean and Proterozoic rocks remobilised during the Neoproterozoic (Abdelsalam et al., 2002).

The Blue Nile and Tekeze-Atbara are sourced in the Ethiopian Highlands, and drain Neoproterozoic arc rocks of the Arabian–Nubian Shield (ANS), Phanerozoic sedimentary rocks, and Cenozoic flood basalts. The ANS is characterised by zircons of juvenile ε_{Hf} composition derived from oceanic arc rocks of 870–630 Ma in age, with some older inherited grains (e.g. Ali et al., 2013; Stern et al., 2010). ε_{Nd} bulk rock values are positive with low $^{87}Sr/^{86}Sr$ ratios (Stern, 2002; Stern and Kroner, 1993). The Phanerozoic cover rocks of the region are partly recycled from the underlying ANS and SMC rocks, and partly from rocks far distant to these underlying basements, as demonstrated by the occurrence of a significant 1000 Ma zircon population unknown from the basements in this region. The Phanerozoic cover sequence is characterised by quartzose sand with durable heavy minerals, a zircon U–Pb age spectrum which typically shows a significant proportion of highly negative ε_{Hf} values at ∼600 and 1000 Ma, and ε_{Nd} and $^{87}Sr/^{86}Sr$ bulk-rock values intermediate between those of cratonic basement and the ANS (Fielding et al., 2017; Morag et al., 2011; Weissbrod and Bogoch, 2007). The Cenozoic Flood Basalts contain bimodal voluminous mafic and more temporally and spatially restricted felsic volcanics; the latter yielded Cenozoic zircons of positive ε_{Hf}, ranging in age between 22 and 33 Ma, with peaks at 25 and 30 Ma (Prave et al., 2016). Positive ε_{Nd} bulk-rock values and low $^{87}Sr/^{86}Sr$ ratios are typical of these juvenile igneous rocks (Fielding et al., 2017; Pik et al., 1999).

Downstream, the modern Nile trunk river receives input from the Red Sea Hills (RSH), which are formed of Phanerozoic sedimentary rocks overlying ANS basement, together with an aeolian contribution. It has also been proposed that, in the past, the Western Desert region may have contributed to the Nile drainage (Issawi and McCauley, 1992). The Western Desert consists of Saharan Metacraton overlain by Phanerozoic sedimentary cover rocks, as described above, and extensive dune sands.

2.3. The Nile's detrital signature today

The detrital signature of the modern Nile river has been documented by Fielding et al. (2017) and references therein. They conclude that there is considerable evolution in the detrital signature of the river downstream, controlled predominantly by changes in local geology and geomorphology. We summarise the conclusions of that work as follows:

For much of its course, the White Nile has an extremely low gradient, crossing an extensive area of marshland in South Sudan, known as the Sudd Marshes. Upstream of the Sudd Marshes, the White Nile is characterised by felspatho-quartzose sand. Detrital zircons are predominantly Archaean, with a small Neoproterozoic population, and have negative ε_{Hf} signatures, reflecting their source in Archaean basement rocks of the Congo–Tanzania Craton. White Nile sediments have negative ε_{Nd} bulk rock values coupled with high $^{87}Sr/^{86}Sr$ ratios (Fielding et al., 2017; Garzanti et al., 2006; Padoan et al., 2011)

In contrast, White Nile sediments north (downstream) of the Sudd in Sudan show derivation from locally-derived Phanerozoic sedimentary cover, and further downstream, input from the Blue Nile-derived Gezira Fan. These observations confirm that very little material makes its way across the Sudd into the downstream trunk Nile.

The detrital zircon signatures of the Blue Nile and Atbara are influenced strongly by their proximity to the Arabian–Nubian Shield, with local influence from cover rocks. Minor contributions of Cenozoic zircons in both rivers demonstrate the presence of zircon-fertile sources within the Ethiopian Flood Basalt province. In contrast, the Sr–Nd isotope signature of Blue Nile and Atbara muds is dominated by input from Ethiopian Flood Basalts.

Zircon age and hafnium isotope characteristics of the modern trunk Nile in northern Egypt show a further shift in signal, with decreasing ANS influence, and are dominated by zircons derived from Phanerozoic cover sedimentary rocks of the Red Sea Hills and modern aeolian and wadi sands. In contrast, the bulk isotopic Sr–Nd–Hf data show little downstream evolution and remain dominated by mafic input from the Ethiopian Highlands in northern Egypt.

3. Analytical methods

Medium sand, silt and mud samples were taken from east, west and central Nile delta cone cores of Oligocene (27.5 and 31 Ma), Miocene (15.2, 15.5 and 17 Ma), Pliocene (2.65–3.25 Ma) and Pleistocene (1.295 Ma) age (Appendix 1). Detailed analytical methods for techniques applied to the Nile delta core samples are given in Appendix 2. Methods are summarised below.

Zircon and rutile grains were separated using standard methods, then hand-picked and mounted in epoxy disks and polished to reveal their interiors. All zircon grains were imaged using cathodoluminescence prior to analysis to allow targeting of laser spots. U–Pb analyses for both zircon and rutile were carried out at the NERC Isotope Geosciences Laboratory (NIGL), using a single collector Nu-Attom mass spectrometer with one of three New Wave laser systems, typically using a 35 μm laser spot. Hafnium isotope composition of zircons was measured at NIGL using a Thermo-Electron Neptune Plus mass spectrometer, coupled to a New Wave 193UC or 193FX Excimer laser. A 50 μm spot was used, targeting previously dated zircon domains.

Plagioclase and white mica were separated from the light fraction remaining after zircon and rutile separation. Ar–Ar analyses were carried out at SUERC, East Kilbride, using a GVi instruments ARGUS 5-collector mass spectrometer using a variable sensitivity Faraday collector array in static collection (non-peak hopping) mode (Mark et al., 2009; Sparks et al., 2008).

Mud samples for Sr, Nd and Hf analysis were leached in dilute acetic acid to remove carbonate before spiking with ^{149}Sm–^{150}Nd, ^{176}Lu–^{180}Hf, ^{87}Rb and ^{84}Sr isotope tracers. Standard dissolution methods and ion-exchange chromatography were used to separate elements of interest. Sr and Nd isotope compositions were measured at NIGL on a Thermo-Electron Triton mass spectrometer, using dynamic multicollection. Hf isotope composition was analysed

in static mode on a Thermo-Electron Neptune mass spectrometer coupled to a Cetac Aridus II desolvating nebuliser.

XRF major element analyses on fused glass disks and trace element analysis in pressed powder pellets was carried out at the Open University in Milton Keynes using a wave-dispersive spectrometer.

Petrographic and heavy mineral analyses of sands and muds were carried out according to Garzanti et al. (2006) and Garzanti and Andò (2007). Split aliquots of each bulk sample were impregnated with Araldite and prepared as standard thin sections and stained with alizarine red to distinguish calcite from dolomite. In each thin section, 400 points were counted for petrography according to the Gazzi–Dickinson method (Ingersoll et al., 1984). Between 200 and 270 transparent heavy minerals were counted in grain mounts by the "area method" (Galehouse, 1971).

4. Results

4.1. U–Pb and Lu–Hf analysis of zircon

Our new data from Saharan dune sands, collected in the Western Desert of Egypt, show that these strongly resemble the underlying Western Desert Phanerozoic cover bedrock in their zircon U–Pb ages and Hf signatures (Figs. 2, 3, 4A, 5). These data were collected in order to complete the source characterisation of Fielding et al. (2017) for the Nile catchment, necessary for a robust comparison with Nile delta samples to be made.

All Nile delta cone sand samples from Oligocene to Pleistocene are dominated by a c. 600 Ma Pan-African peak in zircon age distributions (Fig. 2, Appendix 3). In addition, there are subordinate populations between 630–850 Ma and at c. 1000 Ma. Sparse Archaean and Palaeoproterozoic grains are also present in each sample in different proportions, with Oligocene and Pliocene samples containing a higher proportion of grains >1500 Ma compared to the Miocene and Pleistocene samples. Sparse Cenozoic grains are present in many Oligocene to Pleistocene samples.

Grain populations between 630 and 900 Ma are dominated by arc-like ε_{Hf} signatures ($\varepsilon_{Hf} > 4$). In addition, all samples show significant populations with negative ε_{Hf} values, particularly at c. 600 Ma (Fig. 3, Appendix 4). Sparse grains at c. 1000 Ma show both juvenile and craton-dominated signatures. Palaeoproterozoic and Archaean grains typically have negative ε_{Hf}, with minimum values indicating derivation from c. 3200 Ma crust.

Since U–Pb zircon age spectra are similar in all analysed delta samples, and are dominated by grains of c. 600 Ma, we use hafnium model ages to better discriminate between samples. Hf model ages emphasise the relative input of zircons derived from juvenile ANS arc crust (with model ages between c. 900 and 1300 Ma) and zircons derived directly from, or by melting of, more ancient crustal material (which have model ages >1500 Ma). Nile catchment sources can be discriminated using cumulative probability plots of Hf model ages (Fig. 4A). All delta samples broadly overlap the field defined by Red Sea Hill sedimentary rocks and the modern Nile trunk in Egypt. In detail, the proportion of grains with juvenile rather than crust-dominated Hf model ages is greater in Miocene and Pleistocene samples compared to those from the Oligocene and Pliocene (Fig. 4B). A multidimensional scaling plot (Vermeesch et al., 2016) constructed using hafnium model ages confirms the similarity of delta samples to RSH sedimentary rocks and the modern trunk Nile (Fig. 5).

4.2. U/Pb rutile, $^{40}Ar/^{39}Ar$ mica and plagioclase

Rutile grains from Oligocene to Pleistocene delta sands show a broad distribution in age, ranging from c. 700 to 500 Ma (Appendices 5–7) reflecting a strong Pan-African overprint, and are similar to the age spectra obtained from modern Nile sand and Phanerozoic cover sediment (Avigad et al., 2017; Fielding et al., 2017). Mica and plagioclase Ar–Ar data from Miocene to Pleistocene samples show similar age peaks, with Cenozoic plagioclase grains recorded in the Pliocene sample only. Fresh feldspar was absent in Oligocene samples, so these yielded no usable data.

4.3. Rb/Sr, Sm/Nd and Lu/Hf bulk rock analyses

The majority of delta cone samples define a prominent trend on an Rb–Sr plot (Fig. 6, Appendix 8). This trend extends to significantly more radiogenic $^{87}Sr/^{86}Sr$ values than are seen in modern muds from the Nile River, with values higher than signatures from any known potential source in the Nile catchment.

In addition to bulk analyses, the <2 μm fraction was separated from three Nile cone mud samples, and three Red Sea Hills modern muds. In most cases, <2 μm fractions have significantly higher $^{87}Sr/^{86}Sr$ and $^{87}Rb/^{86}Sr$ than the bulk muds. For the delta muds, the <2 μm analyses plot on an extension of the dominant trend shown by the bulk data (Fig. 6).

On a plot of ε_{Nd} against $^{87}Sr/^{86}Sr$ (Fig. 7), Nile cone data show considerable scatter to the right of a trend defined by mixing between average Ethiopian CFB (Pik et al., 1999) and average Red Sea Hills mud (Fielding et al., 2017). In general, Oligocene and Pliocene samples have higher $^{87}Rb/^{86}Sr$, $^{87}Sr/^{86}Sr$, and lower ε_{Nd} values than Miocene and Pleistocene samples.

On a plot of ε_{Hf} against ε_{Nd} (Fig. 8), the Hf isotope composition of a mafic modern river mud from the Tekeze River (Fielding et al., 2017), which drains the Ethiopian Flood basalts, has been used as an average for the Ethiopian flood basalts. The Tekeze samples have similar isotope compositions to tholeiitic basalts from Ethiopia (Meshesha and Shinjo, 2010) and plot on a steep trend, similar to alkali basalts described by Meshesha and Shinjo (2010) in Ethiopia. The Blue Nile samples plot directly between the mafic end member and the Red Sea Hills muds.

Trace element data were also collected for these samples, as documented in Appendix 10.

4.4. Petrography and heavy mineral analyses

The delta sands range from feldspatho-quartzose to quartzose, containing sparse granitoid lithic fragments and micas, sedimentary lithic fragments (shale, siltstone/sandstone, limestone, dolostone), low-grade metamorphic lithic fragments, and extremely sparse carbonates (<0.3%). Altered volcanic rock fragments are present from the Oligocene base of the studied core upwards, but are only common in the Upper Pliocene and Pleistocene samples. Nevertheless, volcanic detritus in most samples occurs in higher proportions than in Red Sea Hills wadi sands, or in any Saharan samples (Garzanti et al., 2015). Pyroxene is lacking (Fig. 9, Appendix 9).

Analysis of heavy mineral assemblages shows that diagenesis has strongly affected the composition of samples with increasing depth, demonstrated by progressively decreasing transparent heavy mineral concentration index (tHMC; Garzanti and Andò, 2007), and progressively increasing Zircon-Tourmaline-Rutile index (ZTR; Hubert, 1962) (Fig. 9).

5. Interpretations

5.1. Initiation of Nile drainage

The time when the Nile expanded its drainage from one of local catchment to one of continental proportions, stretching as far south as the Ethiopian Highlands, is highly debated. Establishment of a substantial Nile catchment in the Eocene is proposed by
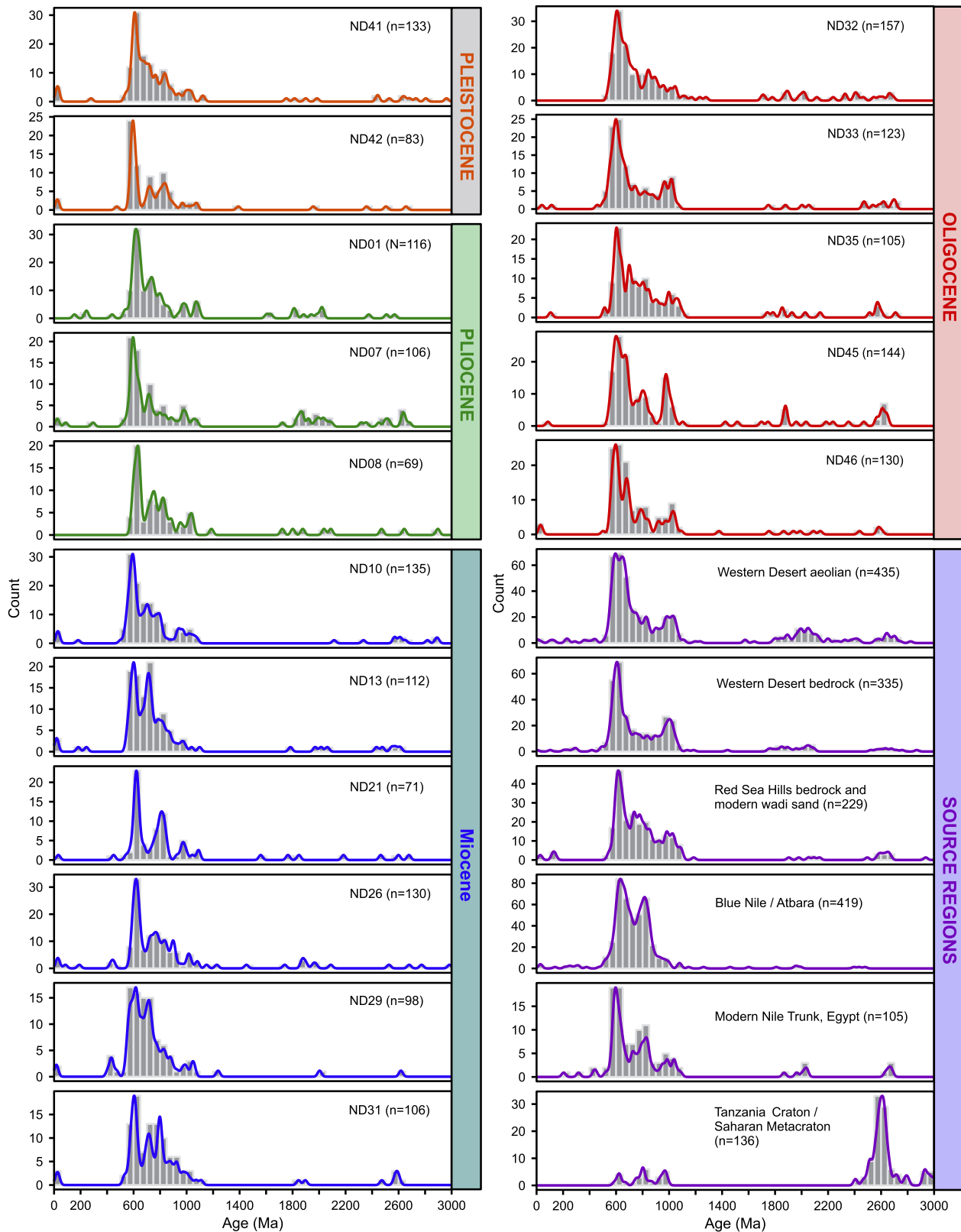
Fig. 2. Detrital zircon U–Pb data for Nile delta samples. Also shown for comparison are signatures for the various possible source regions that potentially contributed to the Nile delta through time (data from Fielding et al., 2017, and references therein, Western Desert aeolian samples are new data and hence shown separately).

Underwood et al. (2013) on the basis of the delta's sedimentary architecture. Proponents of Oligocene initiation of Nile drainage from the Ethiopian plateau used knickpoint facies and thermochronology to infer Oligocene fluvial incision of the plateau (Gani et al., 2007; Pik et al., 2003), but they did not consider downstream palaeodrainage. Conversely, sparse remotely sensed radar data is used to argue for a south-draining system dominating the Nile valley until the Miocene Messinian Salinity Crisis, when drainage flow
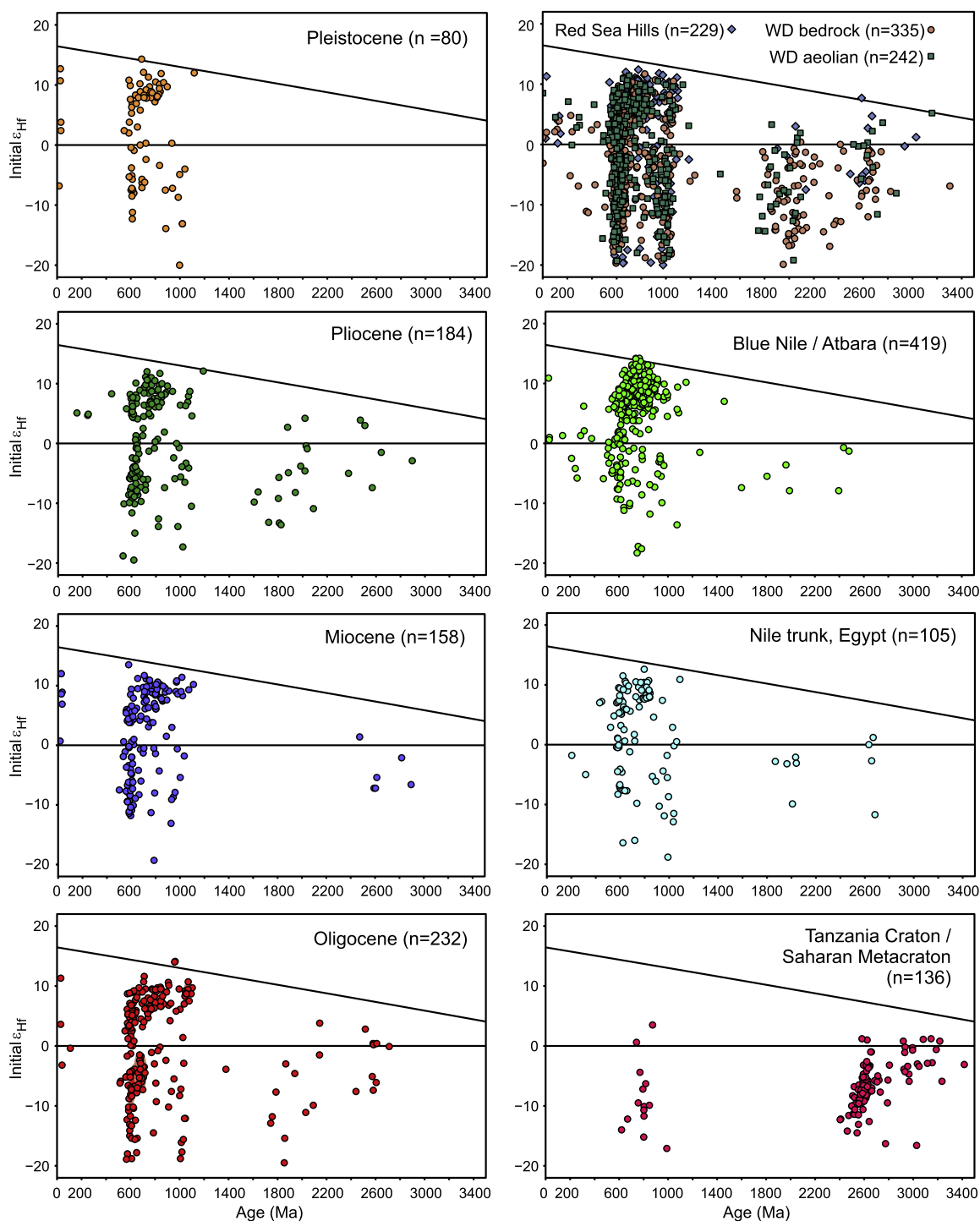
Fig. 3. Lu–Hf data for U–Pb dated detrital zircons from the Nile delta samples. Also shown for comparison are signatures for the various possible source regions that potentially contributed to the Nile delta through time (data from Fielding et al., 2017, and references therein, Western Desert aeolian samples are new data and hence plotted separately).

switched to the north as a result of down-cutting and river capture (Issawi and McCauley, 1992). A connection between the Ethiopian Highlands and the main Nile was not proposed. Volume calculations of delta-cone sediments and the apparent lack of Ethiopian-derived detritus in the delta as determined by heavy-mineral studies have been used to infer that a connection with the Ethiopian Highlands did not occur until the Pleistocene (Macgregor, 2012; Shukri, 1949/1950).

Within the Nile catchment, voluminous Cenozoic volcanic rocks are unique to the Ethiopian Highlands. Thus, first detection of such material in the Nile delta sedimentary record indicates the time at which tectonic and/or climatic changes in North Africa led to the establishment of an extensive drainage network on the scale of the modern Nile.

An early provenance study of the Nile delta (Shukri, 1949/1950) proposed that the river Nile only connected to the Ethiopian Highlands in the mid-Pleistocene, based on the oldest occurrence of volcanic-derived clinopyroxene in samples of that age. However, our combined petrographic and heavy-mineral study shows that diagenesis has led to the breakdown of unstable heavy miner-
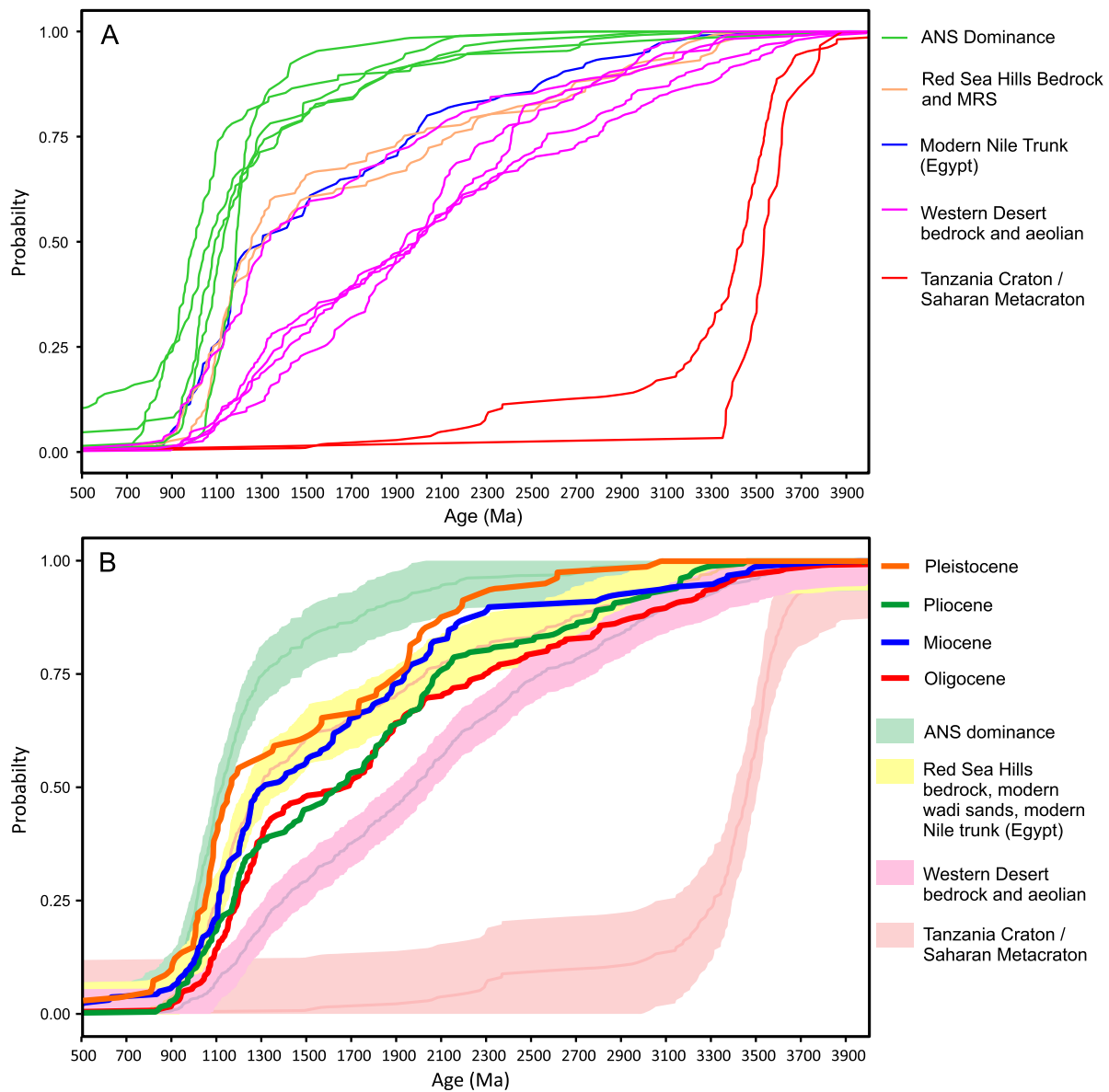
Fig. 4. Cumulative probability plot of Hf model ages. A) shows data from individual samples from potential source regions: green = Arabian Nubian shield as characterised by detritus in Blue Nile and Atbara modern rivers and Hammamat Fm; yellow = RSH, both bedrock and modern wadi sands; pink = Western Desert, both bedrock and aeolian cover; orange = Tanzanian and Saharan Metacratons. Also shown is the Nile Trunk, sample collected from northern Egypt (blue). Data are from Fielding et al. (2017) except for the Western desert aeolian sample which is new. B) shows data from the Nile delta samples, with the source regions now shown as shaded fields corresponding to the same colours as in A).

als, including clinopyroxene, in sediments as young as Pleistocene, with a major increase in ZTR and decrease in tHMC down-section. The absence of clinopyroxene in older sediments cannot therefore be used to indicate the absence of an Ethiopian connection.

Our previous work shows that Cenozoic zircons are only present in the Nile catchment in rivers draining the Ethiopian Highlands. They are absent in White Nile sediments, and modern wadi sediment of the Red Sea Hills, and extremely sparse in dune sand samples from the Western Desert (Fielding et al., 2017 and references therein; Figs. 2 and 10).

In catchment samples, Cenozoic grains derived from the Ethiopian Highlands have a bimodal age distribution corresponding to the two main volcanic episodes of the region, at c. 30–32 Ma and 20–26 Ma (Ukstins et al., 2002). Ethiopian rhyolites from Lake Tana have been dated at c. 31 Ma, and show a range of ε_{Hf} values from +15 to +5. Cenozoic zircons from the modern Blue Nile, Atbara and Tekeze rivers show two populations: c. 30 Ma grains have ε_{Hf} values dominated by less juvenile values (ε_{Hf} +5–0) than the Lake

Tana samples, but showing some grains with a similar composition; 23–27 Ma grains show ε_{Hf} between +3 and +14 (Fig. 10c).

Oligocene and younger samples from the delta cone contain sparse Cenozoic zircons with a similar age distribution to zircons with Ethiopian provenance found in modern Nile sediments, together with a number of younger (15–20 Ma) grains (Fig. 10b, d). The older, Cenozoic grains (c. 31 Ma) in the Nile cone show a similar range in age and ε_{Hf} to zircons carried by the Blue Nile and Atbara. The younger population (c. 26 Ma) plots closer to depleted mantle values than the c. 31 Ma grains, again similar to modern Blue Nile populations.

Sr–Nd bulk analysis of core muds from the Nile delta cone (Fig. 7) show intermediate values between Ethiopian CFB and Red Sea Hills sediments/Saharan aerosols. The simplest explanation for the observed distribution requires a mafic contribution from the Ethiopian Highlands. Nile delta muds could not have been derived from the Red Sea Hills and aeolian sources alone. Derivation of this signature from other Cenozoic mafic sources in Egypt and Sudan
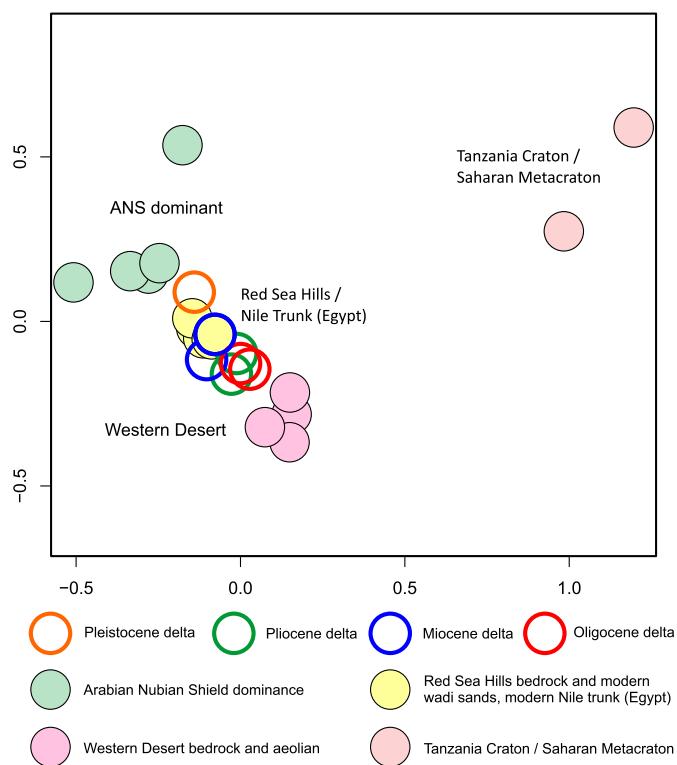
Fig. 5. Multidimensional scaling plot constructed using Hf model ages. Solid circles show individual samples from potential source regions. Open circles show Nile delta data.

(Lucassen et al., 2008) can be ruled out as they are volumetrically insignificant. Models involving simple mixing of average CFB with average Red Sea Hills sources and weathered equivalents (Jung et al., 2004) indicate that the Sr and Nd composition of Oligocene and Pliocene muds could be explained by incorporating 10–20% of CFB, whereas Miocene and Pleistocene muds require 30–45% of mafic input. Our Blue Nile, Atbara and Tekeze sediments plot on the same mixing trends, close to the CFB end-member.

The occurrence of Cenozoic zircons in samples as old as Oligocene, combined with the evidence from Sr and Nd isotopes for input from a mafic end-member in samples of all ages, leads us to conclude that the Nile had expanded to continental proportions, with drainage from the uplifting Ethiopian plateau flowing northwards to the site of the present-day Nile delta, by at least 30 Ma.

5.2. Nile evolution through time

The provenance signature of Nile sediments has remained broadly constant in the Nile delta from Oligocene to the present, with input from the Ethiopian volcanic province documented throughout the cored succession. Similarity in zircon U–Pb age distributions and Hf signature between Nile delta, modern Nile River, and Phanerozoic cover sedimentary rocks illustrates the significance of this source to the delta and the stability of the signal. The availability of >1500 Ma grains in Phanerozoic sedimentary cover in similar proportions to those seen in the delta samples means that it is not necessary to invoke direct derivation of such grains from the White Nile source regions in any samples back to 30 Ma. The absence of a source directly derived from ancient cratonic sources is supported by our hafnium model age and multidimensional scaling plots (Figs. 4, 5). In any case, the White Nile is not thought to have been connected to the main Nile trunk until c. 250 k.y. ago (Williams et al., 2003).

Our Sr and Nd isotope data (Fig. 7) illustrate mixing of an Ethiopian basaltic source with a crustal end member. Aeolian or White Nile sources have commonly been invoked as the crustal end-members in studies of the more recent Nile sedimentary system involving Sr and Nd isotopes (Box et al., 2011; Krom et al., 1999, 2002; Padoan et al., 2011; Revel et al., 2014). Our Nile delta samples span 30 Ma of varying climate, through most of which the White Nile was not connected to the trunk Nile, and aeolian conditions were not prevalent. Our modern Nile and delta samples never show more negative ε_{Nd} values than RSH bedrock and modern wadi sediments, as would be required if Archaean cratonic sources were involved. Furthermore, our data never attain ε_{Nd} values approaching those of Late Holocene Nile delta samples deposited during the Late Holocene aridification of the region, and thus interpreted as comprising a significant component of aeolian input (Revel et al., 2014). We therefore consider locally-derived sediment from the Phanerozoic cover of the Red Sea Hills to be a largely overlooked yet important crustal end member source to the delta mud samples since at least 30 Ma, agreeing with the assertion of Macgregor (2012). This is consistent with the evidence given above for derivation of a significant fraction of zircon grains in Nile delta sands from Phanerozoic cover sequences and is in agreement with the conclusion of Fielding et al. (2017) that the modern Nile trunk contains significant detritus derived from erosion of Phanerozoic cover.

Previous work on silts and muds of the Nile region has demonstrated the influence of grain size on $^{87}Sr/^{86}Sr$ ratios (Garzanti et al., 2013). Both Jung et al. (2004) and Garcon et al. (2014) discuss both the effects of mineralogical sorting and grain size issues on $^{87}Sr/^{86}Sr$ ratios (finer-grained fractions having higher $^{87}Sr/^{86}Sr$ values) as well as the effect of weathering (material subjected to higher degrees of chemical weathering having lower $^{87}Sr/^{86}Sr$ values). Garcon et al. (2014) proposed that facies is also therefore affected by the above processes, with oceanic sediments subject to further fractionation compared to fluvial sediments at the river-ocean interface, resulting in yet higher $^{87}Sr/^{86}Sr$ values. By contrast, Nd isotopic compositions are little affected by the above processes (e.g. Garcon et al., 2013).

In detail, the Sr and Nd isotope data from the Nile delta mud samples show considerable scatter, which we interpret to result from the influence of mineral sorting and grain-size effects. Sr isotope data (Fig. 6) plot on a consistent trend for much of the last 30 Ma, towards a highly radiogenic end-member composition that is not represented by any lithology or source sampled in the catchment area. Comparison of bulk (<63 μm) and <2 μm fractions illustrates that the finer grain-size fractions have elevated $^{87}Rb/^{86}Sr$ and $^{87}Sr/^{86}Sr$ values (Fig. 6). The effect on Nd isotope signature is minimal, with the result that delta mud samples plot to the right of the mixing curve between continental flood basalts and Red Sea Hills sediments in Fig. 7.

A similar degree of scatter is noted in the bulk analyses of ε_{Hf} vs ε_{Nd} (Fig. 8). As with the Sr-Nd data, delta samples can be modelled as a mixture between the two end members of the RSH and the Tekeze River draining the CFBs. We ascribe the scatter to sorting effects, which preferentially affect Hf rather than Nd systems in sedimentary systems (Garcon et al., 2014).

We have argued above for similarity of provenance and thus a stable drainage from Oligocene times onwards. However in detail, subtle differences can be observed between Oligocene and Pliocene Nile cone sediments, on the one hand, and Miocene and Pleistocene sediments on the other. This can be seen best in their zircon U–Pb and Hf model age data (Figs. 2, 4, 5) and Sr-Nd bulk (Fig. 7) characteristics.

Oligocene and Pliocene samples have a greater proportion of zircons with ages >1500 Ma, and more grains with negative ε_{Hf}, resulting in relatively old hafnium model ages (Fig. 4); they also
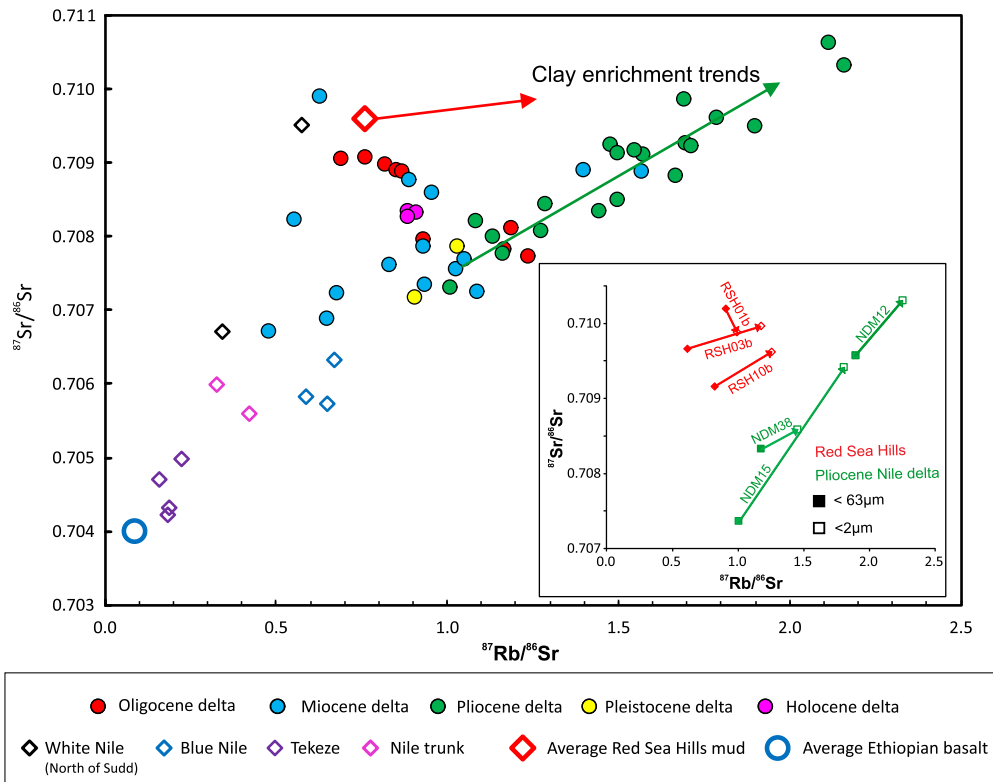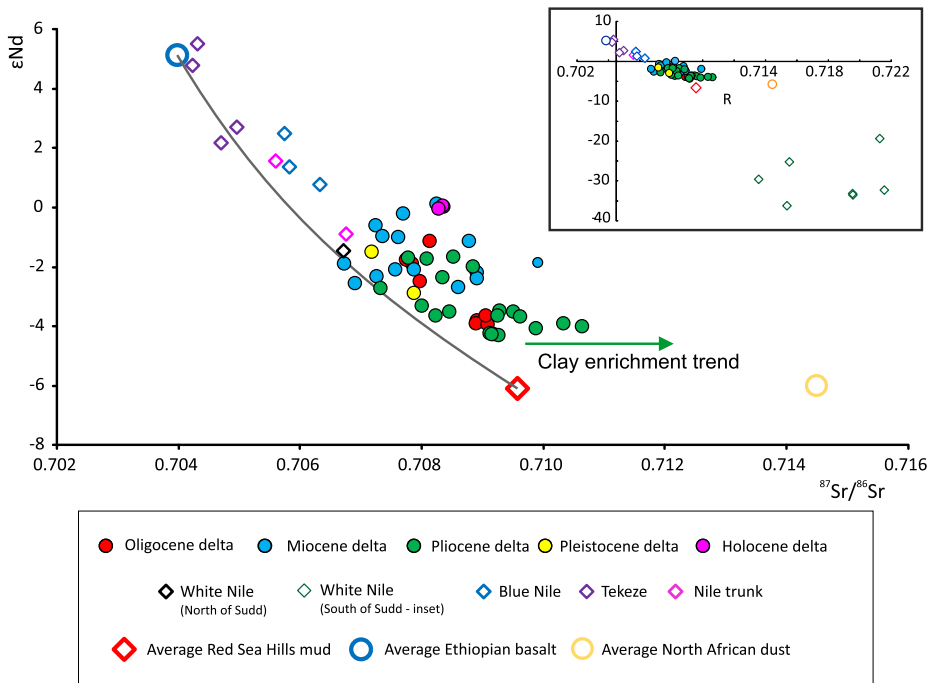
Fig. 6. $^{87}Sr/^{86}Sr$ vs $^{87}Rb/^{86}Sr$ bulk mudstone analyses for Oligocene to modern Nile delta samples. Also shown are values from modern Nile river muds and typical Nile drainage basin signatures (from Pik et al., 1999; Woodward et al., 2015; Fielding et al., 2017). Inset shows comparison of the bulk <63 μm and <2 μm grain size fraction from the same sample; $^{87}Sr/^{86}Sr$ is higher in the finer fraction.

Fig. 7. $^{87}Sr/^{86}Sr$ vs ε_{Nd} bulk mudstone analyses for Oligocene to Modern Nile delta samples. Also shown are values from modern Nile river muds and typical Nile drainage basin signatures (from Pik et al., 1999; Jung et al., 2004; Woodward et al., 2015; Fielding et al., 2017). Solid line shows mixing curve between average Ethiopian CFB value and average RSH signature. R (in inset) shows location of Late Holocene Nile delta data of Revel et al. (2014), interpreted as involving appreciable aeolian input during aridification of the region at this time.

have more evolved Sr–Nd signatures, compared to the Miocene and Pleistocene samples. Variations in the proportions of detritus contributed from different regions of the Nile catchment will reflect tectonic, climatic and geomorphological changes in the region

through time, for example pulsed uplift of the Ethiopian plateau, uplift of the Red Sea Hills, changes in tectonic stresses related to rifting, the Messinian Salinity Crisis, and regional climate change (e.g. Gani et al., 2007 and references therein).
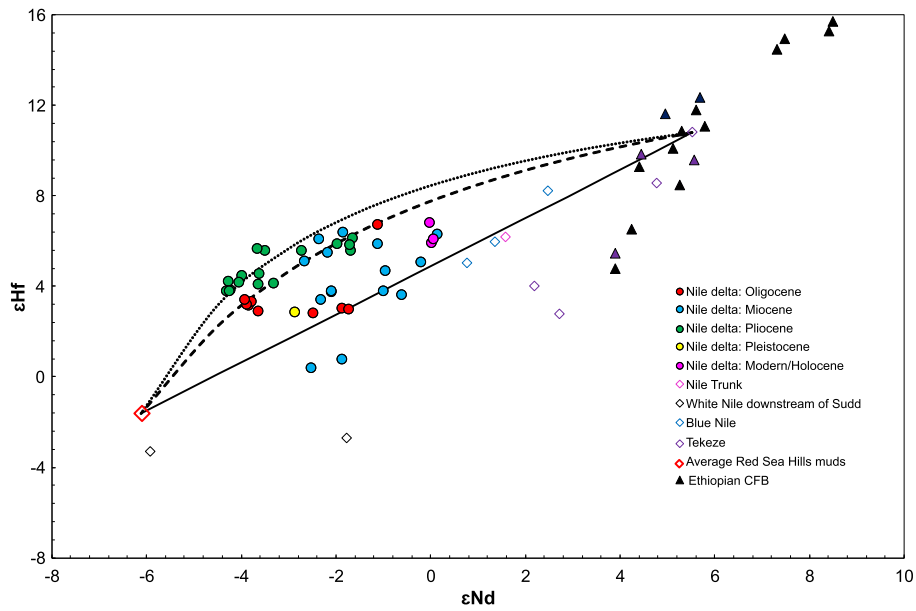
Fig. 8. ε_{Nd} vs ε_{Hf} bulk mudstone analyses for Oligocene to Modern Nile delta samples. Also shown are values from modern Nile river muds and typical Nile drainage basin signatures (data from Meshesha and Shinjo, 2010; Nelson et al., 2012; Fielding et al., 2017). Solid line represents mixing between average Red Sea Hills and CFB-dominated Tekeze River value. Dotted and dashed lines represent the mixing trend for the same two end members for the Pliocene and Oligocene, Miocene and Pliocene, respectively.
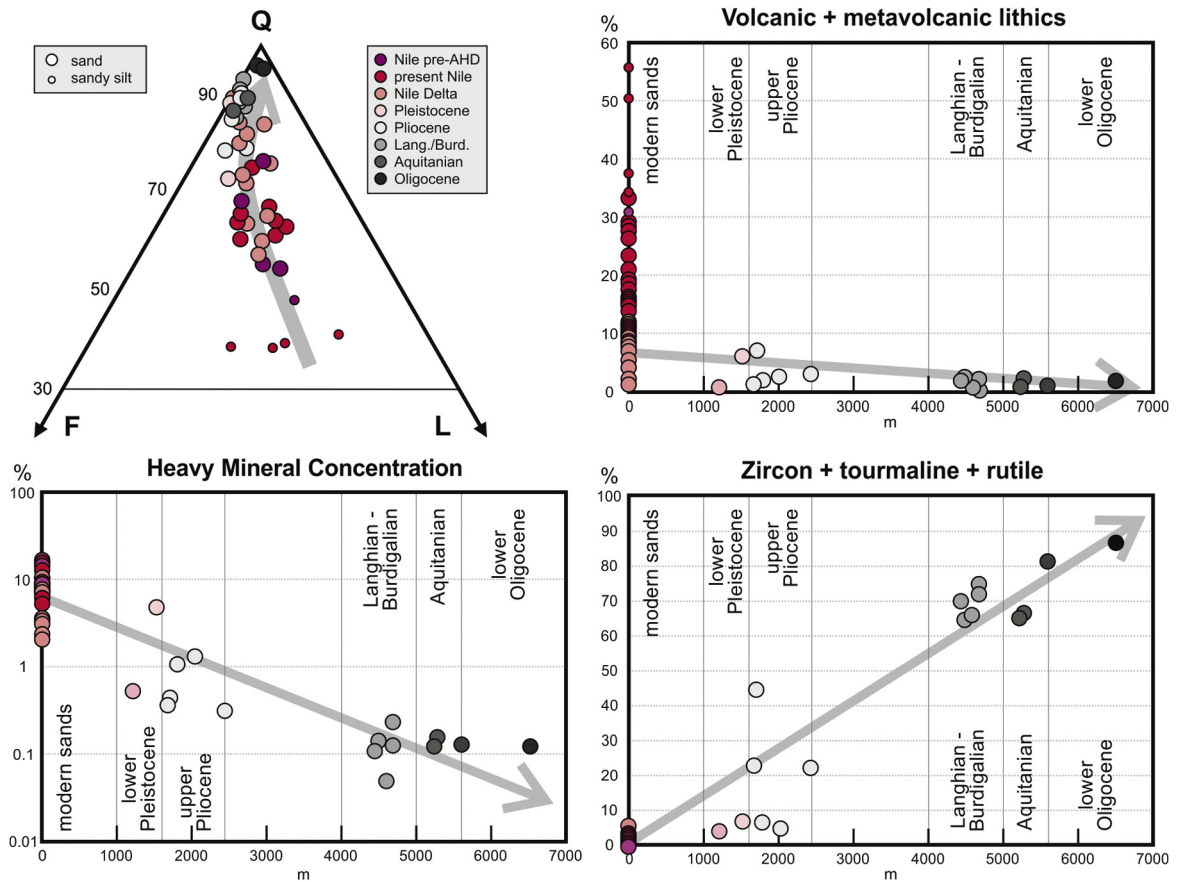

Fig. 9. Downhole compositional trends in the Nile Delta as depicted by petrography and heavy minerals. "m" on X axes are depths in metres. Feldspars (F), lithic fragments of dominantly volcanic origin (L), and unstable heavy minerals all decrease progressively with burial depth, whereas quartz (Q) and durable heavy minerals (ZTR index of Hubert, 1962) relatively increase. Such progressive changes are explained by selective intrastratal dissolution rather than by provenance changes (Andò et al., 2012; Garzanti, 2017).
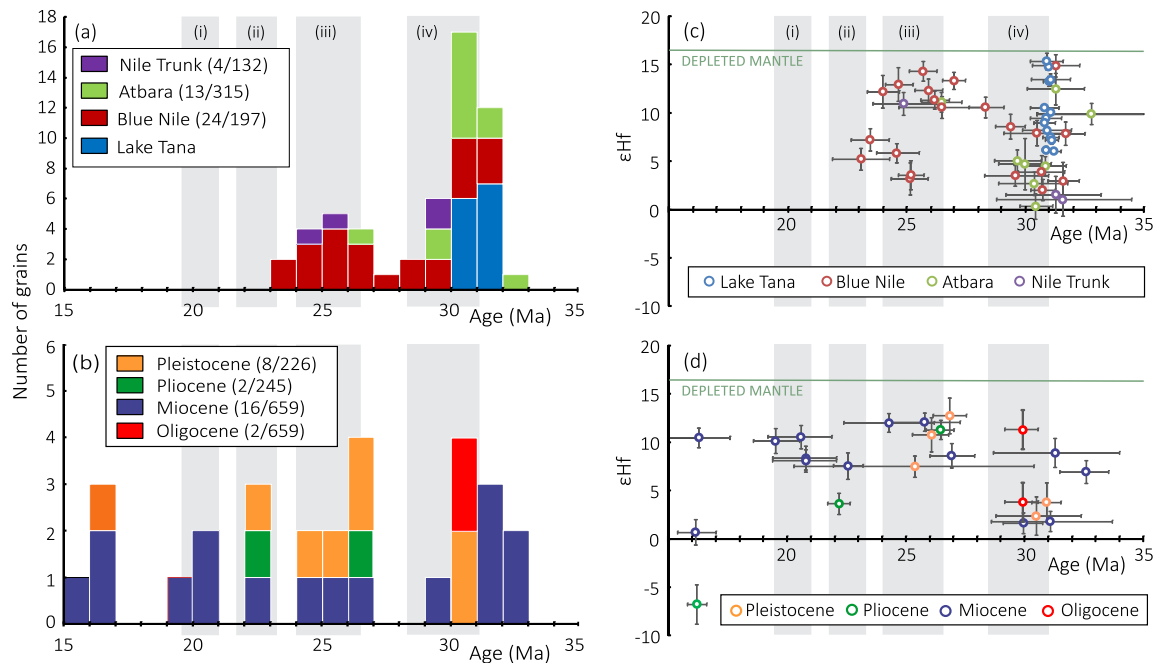
Fig. 10. Cenozoic zircon data from the modern Nile catchment and Nile delta cone. (a) Histograms for Cenozoic detrital zircons from the Nile and its tributaries, together with zircons from Lake Tana rhyolites (ages from Prave et al., 2016). (b) Histograms for detrital zircons in Miocene to Pleistocene Nile cone samples (note two additional grains of 45 Ma were also recorded, not plotted as off-scale). (c) Plot of initial ε_{Hf} values against age for detrital zircons from the modern Nile and its tributaries, together with zircons from the Lake Tana rhyolites. (d) Plot of initial ε_{Hf} values against age for detrital zircons in Miocene to Pleistocene Nile cone samples. Shaded areas (i), (iii) and (iv) represent episodes of volcanism recorded in the Ethiopian Highlands (Ukstins et al., 2002). Shaded area (ii) represents the eruption of the Choke and Guguftu shield volcanos (Kieffer et al., 2004), Numbers in parentheses in the key indicate the number of Cenozoic grains detected in each sample relative to the total number of grains analysed. Note that Cenozoic grains have only been detected in the Nile catchment in rivers draining the Ethiopian Highlands, demonstrating them to be excellent indicators of this provenance; no such grains were detected in the Red Sea Hills modern wadis (0/114) or the White Nile (0/175). One Paleogene grain was detected in Western desert dune sand samples ($n = 435$) but the aeolian nature of this sample precludes further relevant discussion.

6. Wider implications

Data illustrated here provide the first robust evidence of a source-to-sink link from Ethiopian Highlands to Nile Delta since at least the Oligocene, validating the hypotheses of those who proposed an early (Gani et al., 2007; McDougall et al., 1975; Pik et al., 2003; Underwood et al., 2013) rather than late (Issawi and McCauley, 1992; Macgregor, 2012; Shukri, 1949/1950) initiation of this major drainage network.

Initiation and changes of drainage patterns, with their attendant sedimentary records, have long been used as an indirect approach to dating surface uplift (e.g. Cox, 1989) particularly in Africa where the interrelationships between plume influence, continental break-up, epeirogenesis and topographic development are debated (e.g. Paul et al., 2014). Key to understanding the interrelationships are knowledge of the timing of these events. Pik et al. (2003) proposed Blue Nile gorge incision, indicating an uplifted Ethiopian Highlands, since 25–29 Ma, determined from thermochronometry. Paul et al. (2014) used longitudinal river profiles to determine African uplift on the assumption that uplift rate controls profile geometries. They inferred development of Afar topography since 40–35 Ma, although they noted the poor fit between calculated and observed river profiles for Nile tributaries draining the Ethiopian Highlands, which they suggested could be attributed to violation of their assumption of invariant upstream drainage area by river capture. Our research is the first to use a provenance approach to contribute to constraining the timing of this surface uplift. In showing that the Nile routed from the Ethiopian plateau source to delta sink since at least 30 Ma, we infer that the plateau had uplifted by this time, in agreement with studies using alternative approaches (e.g. Moucha and Forte, 2011). An older Ethiopian-sourced Nile might yet be recognised in onshore Eocene deposits (Underwood et al., 2013). Thus it is clear that plateau

uplift occurred early in the continental break-up of the region, preceding the initial stages of Afro-Arabian continental rifting by >5 Ma (Ukstins et al., 2002).

Knowledge of the timing of initiation of the Nile also allows assessment of sapropel formation hypotheses. After closure of the Mediterranean's gateway to the Indian ocean (Karami et al., 2009) sapropels formed in the basin from mid-Miocene times (Kidd et al., 1978; Mourik et al., 2010). Their formation in the Mediterranean is thought to relate to increasing amounts of freshwater reaching the basin by a combination of various factors (increased precipitation versus evaporation, glacial run-off, and discharge from the Nile and other bordering rivers), leading to increased nutrient supply and anoxia promoted by stratification of the water column; the importance of Nile runoff to this process is debated (Krom et al., 2002; Meijer and Tuenter, 2007; Scrivner et al., 2004). It was not previously possible to reconcile models advocating a strong Nile influence on sapropel development with the proposal of a late onset of initiation of major Nile drainage. Now, with the knowledge that the Nile drained into the Mediterranean at least since the Oligocene, a major Nile influence can be invoked, if required, as a major contributor to Mediterranean sapropel development since their first occurrence in the mid-Miocene.

7. Conclusions

Our provenance study on the Oligocene–Recent Nile delta cone sediments documents the evolution of the Nile river and its catchment over time.

The Nile river was established as a major drainage of continental proportions, reaching as far south as the Ethiopian Highlands, by the start of our studied record, in Oligocene times (c. 30 Ma). This is demonstrated by mixture modelling of the delta Sr–Nd data, which shows contribution from the Ethiopian continental

flood basalts from the Oligocene. In addition, Cenozoic zircons derived from felsic volcanic rocks within the Ethiopian Flood Basalt province, are found in delta sediments as old as Oligocene. Initiation of trans-continental Nile drainage by this time constrains the timing of surface uplift of the region and allows further scrutinisation of models of the proposed linkages between Nile run-off and sapropel development.

Previous work (Fielding et al., 2017) showed that Phanerozoic cover sequences contributed a considerable proportion of detritus to the modern trunk Nile river with additional input from the Ethiopian Flood Basalts. Whilst our Sr–Nd and zircon U–Pb and Hf data show subtle variations between Oligocene and Pliocene samples compared to the Miocene and Pleistocene samples, suggesting some variation in the drainage, overall all Oligocene to Pleistocene Nile delta cone samples analysed in this study have similar zircon age/Hf isotope characteristics to modern Nile trunk samples, indicating no major changes in palaeodrainage from Oligocene times to present.

Acknowledgements

Appendix A. Supplementary material

Supplementary material related to this article can be found online at https://doi.org/10.1016/j.epsl.2018.02.031.

References

Abdelsalam, M.G., Liégeois, J.-P., Stern, R.J., 2002. The Saharan metacraton. J. Afr. Earth Sci. 34, 119–136.

Ali, K.A., Wilde, S.A., Stern, R.J., Moghazi, A.K.M., Ameen, S.M.M., 2013. Hf isotopic composition of single zircons from Neoproterozoic arc volcanics and post-collision granites, Eastern Desert of Egypt: implications for crustal growth and recycling in the Arabian–Nubian Shield. Precambrian Res. 239, 42–55.

Andò, S., Garzanti, E., Padoan, M., Limonta, M., 2012. Corrosion of heavy minerals during weathering and diagenesis: a catalog for optical analysis. Sediment. Geol. 280, 165–178.

Avigad, D., Morag, N., Abbo, A., Gerdes, A., 2017. Detrital rutile U–Pb perspective on the origin of the great Cambro-Ordovician sandstone of North Gondwana and its linkage to orogeny. Gondwana Res. 51, 17–29.

Bosworth, W., El-Hawat, A.S., Helgeson, D.E., Burke, K., 2008. Cyrenaican "shock absorber" and associated inversion strain shadow in the collision zone of northeast Africa. Geology 36, 695–698.

Bosworth, W., Huchon, P., McClay, K., 2005. The Red Sea and Gulf of Aden Basins. J. Afr. Earth Sci. 43, 334–378.

Box, M.R., Krom, M.D., Cliff, R.A., Bar-Matthews, M., Almogi-Labin, A., Ayalon, A., Paterne, M., 2011. Response of the Nile and its catchment to millennial-scale climatic change since the LGM from Sr isotopes and major elements of East Mediterranean sediments. Quat. Sci. Rev. 30, 431–442.

Cox, K.G., 1989. The role of mantle plumes in the development of continental drainage patterns. Nature 342, 4.

Craig, T., Jackson, J., Priestley, K., McKenzie, D., 2011. Earthquake distribution patterns in Africa: their relationship to variations in lithospheric and geological structure, and their rheological implications. Geophys. J. Int. 185, 403–434.

Dolson, J.C., Shann, M.V., Matbouly, S., Harwood, C., Rashed, R., Hammouda, H., 2001. The petroleum potential of Egypt. In: AAPG Memoir, vol. 74. Chapter 23.

Ebinger, C., 2005. Continental break-up: the East African perspective. Astron. Geophys. 46, 2.16–12.21.

Fielding, L., Najman, Y., Millar, I., Butterworth, P., Ando, S., Padoan, M., Barfod, D., Kneller, B., 2017. A detrital record of the Nile River and its catchment. J. Geol. Soc. 174, 301–317.

Freydier, R., Michard, A., De Lange, G., Thomson, J., 2001. Nd isotopic compositions of Eastern Mediterranean sediments: tracers of the Nile influence during sapropel S1 formation? Mar. Geol. 177, 45–62.

Galehouse, J.S., 1971. Point counting. In: Procedures in Sedimentary Petrology, pp. 385–407.

Gani, N.D.S., Gani, M.R., Abdelsalam, M.G., 2007. Blue Nile incision on the Ethiopian Plateau: pulsed plateau growth, Pliocene uplift, and hominin evolution. GSA Today 17, 4–11.

Garcon, M., Chauvel, C., France-Lanord, C., Huyghe, P., Lave, J., 2013. Continental sedimentary processes decouple Nd and Hf isotopes. Geochim. Cosmochim. Acta 121, 177–195.

Garcon, M., Chauvel, C., France-Lanord, C., Limonta, M., Garzanti, E., 2014. Which minerals control the Nd–Hf–Sr–Pb isotopic compositions of river sediments? Chem. Geol. 364, 42–55.

Gardosh, M.A., Druckman, Y., Buchbinder, B., 2009. The Late Tertiary deep-water siliciclastic system of the Levant Margin — an emerging play offshore Israel. American Association of Petroleum Geologists Search and Discovery Article 10211.

Garzanti, E., 2017. The maturity myth in sedimentology and provenance analysis. J. Sediment. Res. 87, 353–365.

Garzanti, E., Andò, S., 2007. Heavy mineral concentration in modern sands: implications for provenance interpretation. Dev. Sedimentol. 58, 517–545.

Garzanti, E., Ando, S., Padoan, M., Vezzoli, G., El Kammar, A., 2015. The modern Nile sediment system: processes and products. Quat. Sci. Rev. 130, 9–56.

Garzanti, E., Andò, S., Vezzoli, G., Ali Abdel Megid, A., El Kammar, A., 2006. Petrology of Nile River sands (Ethiopia and Sudan): sediment budgets and erosion patterns. Earth Planet. Sci. Lett. 252, 327–341.

Garzanti, E., Padoan, M., Setti, M., Najman, Y., Peruta, L., Villa, I.M., 2013. Weathering geochemistry and Sr–Nd fingerprints of equatorial upper Nile and Congo muds. Geochem. Geophys. Geosyst. 14, 292–316.

Guiraud, R., Bosworth, W., Thierry, J., Delplanque, A., 2005. Phanerozoic geological evolution of Northern and Central Africa: an overview. J. Afr. Earth Sci. 43, 83–143.

Hamann, Y., Ehrmann, W., Schmiedl, G., Kruger, S., Stuut, J.B., Kuhnt, T., 2008. Sedimentation processes in the Eastern Mediterranean Sea during the Late Glacial and Holocene revealed by end-member modelling of the terrigenous fraction in marine sediments. Mar. Geol. 248, 97–114.

Hubert, J.F., 1962. A zircon-tourmaline-rutile maturity index and the interdependence of the composition of heavy mineral assemblages with the gross composition and texture of sandstones. J. Sediment. Res. 32.

Ingersoll, R.V., Fullard, T.F., Ford, R.L., Grimm, J.P., Pickle, J.D., Sares, S.W., 1984. The effect of grain size on detrital modes; a test of the Gazzi–Dickinson point-counting method. J. Sediment. Res. 54, 103–116.

Issawi, B., McCauley, J.F., 1992. The Cenozoic rivers of Egypt: the Nile problem. In: Adams, B., Friedman, R. (Eds.), The Followers of Horus. Oxbow Press, Oxford, pp. 1–18.

Jung, S.J.A., Davies, G.R., Ganssen, G.M., Kroon, D., 2004. Stepwise Holocene aridification in NE Africa deduced from dust-borne radiogenic isotope records. Earth Planet. Sci. Lett. 221, 27–37.

Karami, M., Meijer, P.T., Dijkstra, H., Wortel, M., 2009. An oceanic box model of the Miocene Mediterranean Sea with emphasis on the effects of closure of the eastern gateway. Paleoceanography 24.

Kidd, R.B., Cita, M.B., Ryan, W.B.F., 1978. Stratigraphy of Eastern Mediterranean sapropel sequences recovered during DSDP 42A and paleoenvironmental significance. Init. Rep. DSDP 42, 22.

Kieffer, B., Arndt, N., Lapierre, H., Bastien, F., Bosch, D., Pecher, A., Yirgu, G., Ayalew, D., Weis, D., Jerram, D.A., Keller, F., Meugniot, C., 2004. Flood and Shield Basalts from Ethiopia: magmas from the African Superswell. J. Petrol. 45, 793–834.

Klitzsch, E.H., Squyres, C.H., 1990. Paleozoic and Mesozoic geological history of North Eastern Africa based upon new interpretation of Nubian strata. Am. Assoc. Pet. Geol. Bull. 74, 8.

Krom, M., Cliff, R., Eijsink, L., Herut, B., Chester, R., 1999. The characterisation of Saharan dusts and Nile particulate matter in surface sediments from the Levantine basin using Sr isotopes. Mar. Geol. 155, 319–330.

Krom, M.D., Stanley, J.D., Cliff, R.A., Woodward, J.C., 2002. Nile River sediment fluctuations over the past 7000 yr and their key role in sapropel development. Geology 30, 71–74.

Kröner, A., Stern, R., 2004. Africa: Pan-African orogeny. In: Encyclopedia of Geology. Elsevier, pp. 1–12.

Lucassen, F., Franz, G., Romer, R.L., Pudlo, D., Dulski, P., 2008. Nd, Pb, and Sr isotope composition of Late Mesozoic to Quaternary intra-plate magmatism in NE-Africa (Sudan, Egypt): high-μ signatures from the mantle lithosphere. Contrib. Mineral. Petrol. 156, 765–784.

Macgregor, D.S., 2012. The development of the Nile drainage system: integration of onshore and offshore evidence. Pet. Geosci. 18, 417–431.

Mark, D., Barfod, D., Stuart, F., Imlach, J., 2009. The ARGUS multicollector noble gas mass spectrometer: performance for $^{40}Ar/^{39}Ar$ geochronology. Geochem. Geophys. Geosyst. 10.

McDougall, I., Morton, W.H., Williams, M.A.J., 1975. Age and rates of denudation of Trap Series basalts at Blue Nile Gorge, Ethiopia. Nature 254, 207–209.

Meijer, P.T., Tuenter, E., 2007. The effect of precession-induced changes in the Mediterranean freshwater budget on circulation at shallow and intermediate depth. J. Mar. Syst. 68, 349–365.

Meshesha, D., Shinjo, R., 2010. Hafnium isotope variations in Bure volcanic rocks from the northwestern Ethiopian volcanic province: a new insight for mantle source diversity. J. Mineral. Petrol. Sci. 105, 101–111.

Morag, N., Avigad, D., Gerdes, A., Belousova, E., Harlavan, Y., 2011. Detrital zircon Hf isotopic composition indicates long-distance transport of North Gondwana Cambrian–Ordovician sandstones. Geology 39, 955–958.

Moucha, R., Forte, A.M., 2011. Changes in African topography driven by mantle convection. Nat. Geosci. 4, 707–712.

Mourik, A., Bijkerk, J., Cascella, A., Hüsing, S., Hilgen, F., Lourens, L., Turco, E., 2010. Astronomical tuning of the La Vedova High Cliff Section (Ancona, Italy)—implications of the middle Miocene climate transition for Mediterranean sapropel formation. Earth Planet. Sci. Lett. 297, 249–261.

Nelson, W.R., Furman, T., van Keken, P.E., Shirey, S.B., Hanan, B.B., 2012. Os–Hf isotopic insight into mantle plume dynamics beneath the East African Rift System. Chem. Geol. 320, 66–79.

Omar, G.I., Steckler, M.S., 1995. Fission track evidence on the initial rifting of the Red Sea: two pulses, no propagation. Science 270, 1341–1344.

Padoan, M., Garzanti, E., Harlavan, Y., Villa, I.M., 2011. Tracing Nile sediment sources by Sr and Nd isotope signatures (Uganda, Ethiopia, Sudan). Geochim. Cosmochim. Acta 75, 3627–3644.

Paul, J.D., Roberts, G.G., White, N., 2014. The African landscape through space and time. Tectonics.

Pik, R., Deniel, C., Coulon, C., Yirgu, G., Marty, B., 1999. Isotopic and trace element signatures of Ethiopian flood basalts: evidence for plume–lithosphere interactions. Geochim. Cosmochim. Acta 63, 2263–2279.

Pik, R., Marty, B., Carignan, J., Lave, J., 2003. Stability of the Upper Nile drainage network (Ethiopia) deduced from (U–Th)/He thermochronometry: implications for uplift and erosion of the Afar plume dome. Earth Planet. Sci. Lett. 215, 73–88.

Prave, A., Bates, C.R., Donaldson, C.H., Toland, H., Condon, D., Mark, D., Raub, T.D., 2016. Geology and geochronology of the Tana Basin, Ethiopia: LIP volcanism, super eruptions, and Eocene–Oligocene environmental change. Earth Planet. Sci. Lett. 44, 1–8.

Revel, M., Colin, C., Bernasconi, S., Combourieu-Nebout, N., Ducassou, E., Grousset, F.E., Rolland, Y., Migeon, S., Bosch, D., Brunet, P., 2014. 21,000 years of Ethiopian African monsoon variability recorded in sediments of the western Nile deep-sea fan. Reg. Environ. Change 14, 1685–1696.

Salem, R., 1976. Evolution of Eocene–Miocene sedimentation patterns in parts of Northern Egypt. Am. Assoc. Pet. Geol. Bull. 60, 34–64.

Scrivner, A.E., Vance, D., Rohling, E.J., 2004. New neodymium isotope data quantify Nile involvement in Mediterranean anoxic episodes. Geology 32, 565.

Shukri, N.M., 1949/1950. The mineralogy of some Nile sediments. Q. J. Geol. Soc. Lond. 106, 466–467.

Sparks, R.S.J., Folkes, C.B., Humphreys, M.C., Barfod, D.N., Clavero, J., Sunagua, M.C., McNutt, S.R., Pritchard, M.E., 2008. Uturuncu volcano, Bolivia: volcanic unrest due to mid-crustal magma intrusion. Am. J. Sci. 308, 727–769.

Stern, R.J., 2002. Crustal evolution in the East African Orogen: a neodymium isotopic perspective. J. Afr. Earth Sci. 34, 109–117.

Stern, R.J., Ali, K.A., Liegeois, J.P., Johnson, P.R., Kozdroj, W., Kattan, F.H., 2010. Distribution and significance of Pre-Neoproterozoic zircons in juvenile Neoproterozoic igneous rocks of the Arabian Nubian Shield. Am. J. Sci. 310, 791–811.

Stern, R.J., Kroner, A., 1993. Late Precambrian crustal evolution in NE Sudan – isotopic and geochronological constraints. J. Geol. 101, 555–574.

Ukstins, I.A., Renne, P.R., Wolfenden, E., Baker, J., Ayalew, D., Menzies, M., 2002. Matching conjugate volcanic rifted margins: $^{40}Ar/^{39}Ar$ chrono-stratigraphy of pre-and syn-rift bimodal flood volcanism in Ethiopia and Yemen. Earth Planet. Sci. Lett. 198, 289–306.

Underwood, C.J., King, C., Steurbaut, E., 2013. Eocene initiation of Nile drainage due to East African uplift. Palaeogeogr. Palaeoclimatol. Palaeoecol. 392, 138–145.

Vermeesch, P., Resentini, A., Garzanti, E., 2016. An R package for statistical provenance analysis. Sediment. Geol. 336, 14–25.

Weissbrod, T., Bogoch, R., 2007. Distribution plan and provenance implications of the heavy minerals in Neoproterozoic to Mesozoic siliciclastic successions in the Arabo-Nubian Shield and its northern periphery: a review. Dev. Sedimentol. 58, 647–676.

Williams, M.A.J., Adamson, D., Prescott, J.R., Williams, F.M., 2003. New light on the age of the White Nile. Geology 31, 1001–1004.

Woodward, J., Macklin, M., Fielding, L., Millar, I., Spencer, N., Welsby, D., Williams, M., 2015. Shifting sediment sources in the world's longest river: a strontium isotope record for the Holocene Nile. Quat. Sci. Rev. 130, 124–140.